Chinese Journal of
POLYMER SCIENCE

RESEARCH ARTICLE

https://doi.org/10.1007/s10118-026-3641-6
Chinese J. Polym. Sci. **2026**, *44*, 2258–2268

Activated Carbon-derived Polyester Elastomer Foams with Tailored Structure and Blackness for High-performance Thermally Insulating Applications

Xu-Jiang Sun[a,b], Yan-Ru Zhang[a,b], Jia-Peng Ma[c], Xu Wang[d], Ke-Jian Cui[d], Ting-Ting Feng[a,b], and Gui-Long Wang[a,b*]

[a] *State key Laboratory of Advanced Equipment and Technology for Metal Forming; Shandong University, Jinan 250061, China*
[b] *Key Laboratory for Liquid-Solid Structural Evolution and Processing of Materials (Ministry of Education), Shandong University, Jinan 250061, China*
[c] *Shandong Special Equipment Inspection Institute Group Co., Ltd., Jinan 250199, China*
[d] *Shoe Research and Development Innovation System; Li Ning (China) Sports Goods Co., Ltd., Beijing 101111, China*

Electronic Supplementary Information

Abstract Lightweight materials are essential for advanced green manufacturing and ecological sustainability because they reduce energy consumption, minimize pollution, and improve resource utilization. Herein, a reinforcement strategy utilizing activated carbon (AC) as a functional filler to enhance the foaming behavior of thermoplastic polyester elastomer (TPEE) was developed, enabling the successful fabrication of lightweight, high-strength, and elastic TPEE/AC foams with superior hydrophobic and thermally insulating performance using environmentally friendly microcellular foaming technology. The uniform dispersion of AC enhanced the melt strength and the solubility of CO_2, thereby significantly improving the foaming behavior, resulting in refined cell structures and reduced shrinkage. The optimized T-A-5 foam achieved a high expansion ratio (16.0), low shrinkage ratio (70.0%), and high recovery ratio (79.4%), outperforming the pure TPEE foam by 15.9%, 12.3%, and 212.6%, respectively. Moreover, the viscoelastic properties of TPEE/AC composites tested under two different conditions revealed contrasting trends in loss factor, indicating that the influence of fillers on TPEE viscoelasticity is highly temperature-dependent and state-sensitive. Further, the lightness and blackness of TPEE/AC foams can be tailored by varying AC content and cellular morphology. Moreover, the TPEE/AC foams exhibited improved compressive strength, low thermal conductivity (35.9 $mW{\cdot}m^{-1}{\cdot}K^{-1}$), and high hydrophobicity (122.5°). This study provides an effective strategy for designing high-performance TPEE foams with significant potential for energy-saving and environment-friendly applications.

Keywords TPEE foam; Activated carbon; Microcellular foam; Blackness; Thermal insulation

Citation: Sun, X. J.; Zhang, Y. R.; Ma, J. P.; Wang, X.; Cui, K. J.; Feng, T. T.; Wang, G. L. Activated carbon-derived polyester elastomer foams with tailored structure and blackness for high-performance thermally insulating applications. *Chinese J. Polym. Sci.* **2026**, *44*, 2258–2268.

INTRODUCTION

Thermoplastic polyester elastomer (TPEE) is a novel thermoplastic material that typically consists of crystalline blocks with high melting points and amorphous blocks with relatively low glass transition temperatures.[1,2] In this structure, the crystalline polyester segments act as hard blocks, which provide physical crosslinking sites for TPEE, enhancing the strength, temperature resistance, and impact resistance of the material.[3,4] Additionally, the soft segments are primarily composed of aliphatic polyester and polyether, imparting superior elasticity and enhanced low-temperature flexibility.[5] Due to these excellent properties, TPEE demonstrates a wide spectrum of applications, including telecommunications equipment, automotive manufacturing, and aerospace.[6,7]

Research on lightweight, functionalized, and high-performance polymers has become a crucial driving force for modern industrial transformation. Compared to solid TPEE, TPEE microcellular foam exhibits superior characteristics such as light weight, material efficiency, high resilience, high specific strength, thermal insulation, hydrophobicity, and sound absorption.[8,9] These characteristics create unique application prospects in impact absorption, vibration damping, biomedical devices, aerospace and military applications, positioning it as a promising replacement for conventional foam materials.[10] Microcellular foaming technology is an environmentally friendly processing method with low cost and simple processing, serving as an attractive option for producing TPEE microcellular foams.[11–15] However, TPEE exhibits a low melt strength, which results in poor foaming behavior, ultimately limiting the progress in lightweight and functional materials. Furthermore, the severe shrinkage behavior of the

* Corresponding author, E-mail: guilong@sdu.edu.cn
Received January 30, 2026; Accepted March 2, 2026; Published online May 14, 2026

© Chinese Chemical Society
Institute of Chemistry, Chinese Academy of Sciences

TPEE foam also restricts its practical applications.[16,17]

In response to the aforementioned challenges, numerous researchers have made extensive efforts to improve the foaming and shrinkage behavior of TPEE. One approach involves optimizing the foaming process. Xu *et al*. developed high expansion ratio TPEE foams with shrinkage resistant using a supercritical carbon dioxide ($scCO_2$) and nitrogen (N_2) co-foaming strategy.[17] Their study demonstrated that N_2 could reduce the influence of pressure differentials on cell morphology, thereby mitigating foam shrinkage. Other studies have shown that increasing the proportion of hard segments in TPEE molecular chains enhances the foam's resistance to shrinkage. A higher hard segment proportion can strengthen the polymer matrix, enabling it to better withstand the negative pressure gradients, thereby preserving dimensional stability.[9] Additionally, the incorporation of micro/nano fillers or a second polymer phase has proven effective in enhancing the foaming and shrinkage behavior of TPEE. Fillers such as silica, graphite nanoplates and carbon nanotubes have been widely studied in this regard.[18–22] In recent years, activated carbon (AC) has garnered increasing attention in both academia and industry due to its abundant porous morphology, low cost, high specific surface area, and excellent strength. These features make AC a promising candidate for improving the foam structure and enhancing the overall performance of polymeric elastomer foams.

In this study, lightweight, highly elastic, shrinkage-resistant, thermally insulating, and hydrophobic TPEE/AC foams were successfully fabricated using a green, cost-effective, and facile microcellular foaming technology. First, the dispersion of AC in the TPEE matrix and its influence on the thermal behavior of TPEE were investigated. Second, the rheological and dynamic thermomechanical properties of TPEE/AC composites were systematically investigated. Subsequently, the effects of AC content on the foaming behavior and shrinkage recovery of the composites were systematically examined. Finally, the blackness, compressive mechanical properties, thermal insulation, and hydrophobicity of the composite foams were evaluated, along with a comprehensive analysis of how the AC content and cell structure influence foam performance. This study proposes a novel strategy for fabricating lightweight, high-performance materials, which is of great significance for lightweight applications, lowering energy usage, and promoting environmental sustainability.

EXPERIMENTAL

Materials

Thermoplastic polyester elastomer (TPEE) pellets were 4056 from DuPont, USA. Its density, melting temperature, and Shore hardness were 1.16 g·cm^{-3}, 152 °C, and 43D, respectively. Activated carbon (AC) was C829813 from the Shanghai McLean Biochemical Technology Co., Ltd. The average particle size is 38 μm.

Fabrication of TPEE/AC Foams

Before blending, the TPEE pellets and AC were pre-dried at 90 °C for 8 h to remove any absorbed moisture. Fig. 1 presents the preparation process of TPEE/AC composites and foams. TPEE/AC mixtures with varying AC contents (0 wt%, 1 wt%, 3 wt%, 5 wt%, and 10 wt%) were initially mixed with a glass rod. Subsequently, the mixtures were added into an internal mixer to melt blending. The operational parameters of the internal mixer were as follows: a rotational speed of 50 r·min^{-1}, a temperature of 165 °C, and a processing time of 8 min. The blends were subjected to hot pressing on plates with a thickness of 4 mm.

To investigate the effects of temperature and pressure on the experimental results, the foaming temperature was set in the range of 115–140 °C, applying different foaming pressures, and maintaining a saturation time of 50 min. TPEE/AC foams were labeled as T-A-*a*, where *a* denotes the weight percentage of AC in the composites.

Characterizations

The characterizations and measurements are shown in electronic supplementary information (ESI).

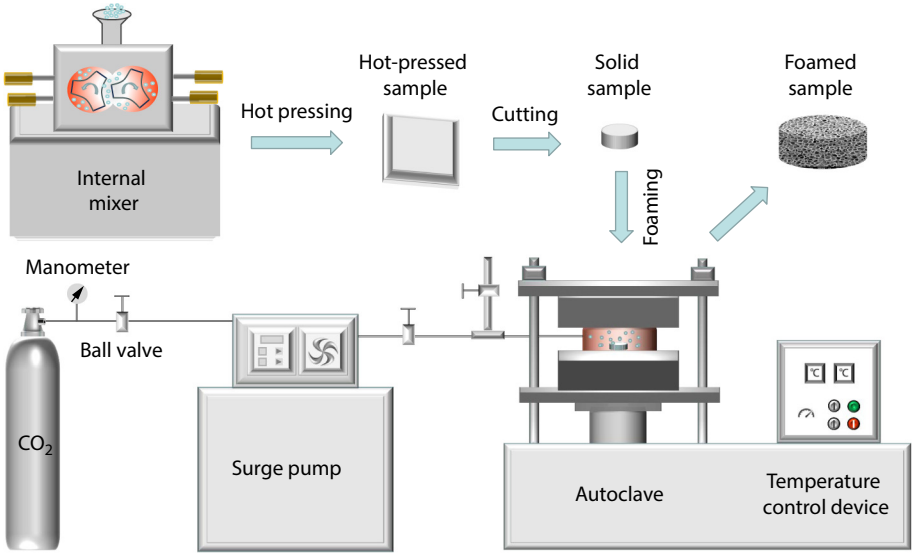

Fig. 1 The preparation of TPEE/AC foams.

https://doi.org/10.1007/s10118-026-3641-6

RESULTS AND ANALYSIS

Phase Morphology and Thermal Behavior

The effective dispersion of fillers throughout the polymer matrix is key to enhancing mechanical properties and controlling the foaming behavior. Figs. 2(a)–2(f) illustrate the phase morphology of AC and the dispersion of varying content of AC within the TPEE matrix, respectively. It can be observed that due to the electrostatic effect of the AC particles, their initial size ranges from 1 μm to 5 μm. After melt blending, under strong shear forces and the encapsulation effect of TPEE molecular chains, the AC particles undergo fragmentation and are uniformly dispersed within the TPEE matrix, with particle sizes reduced to approximately 40–200 nm. Moreover, increasing AC content leads to higher apparent density and larger average size of AC in the TPEE matrix, with minor agglomeration occurring. Nevertheless, AC remains relatively well dispersed throughout the matrix. Furthermore, no obvious interfacial separation between the AC and TPEE is observed, indicating a good interfacial adhesion between the dispersed AC and the TPEE. Figs. 2(g) and 2(h) present the first cooling curves and second heating curves of the TPEE/AC composites obtained from DSC, respectively. As shown in Fig. 2(g), the crystallization temperature of TPEE during the cooling process is 87.8 ℃. With increasing AC content, the crystallization peak gradually shifts toward higher temperatures, indicating an accelerated crystallization process. This behavior can be ascribed to the high specific surface area of AC, which provides strong adsorption sites for TPEE molecular chains.[23,24] This interaction restricts the chain mobility and reduces the nucleation energy barrier, thus facilitating earlier crystallization. Moreover, as shown in Fig. 2(h), the melting point of TPEE during heating process is 150.4 ℃. The melting temperature of TPEE/AC composites slightly increases as the AC content increases. The increase may result from the porous structure of AC, which exhibits an adsorption effect on TPEE molecular chains, restricting their mobility. Such restriction promotes the crystallization of the hard segments, thereby leading to an elevated melting temperature. The relevant DSC data are provided in ESI.

Rheological Behavior and Dynamic Thermodynamic Analysis

Rheological behavior is one of the key factors influencing the foaming behavior of thermoplastic polymers. Figs. 3(a)–3(c) present the relationships between the storage modulus (G'), loss modulus (G''), complex viscosity (η^*), and loss tangent (tanδ) with angular frequency (ω) for TPEE/AC composites. As shown in Fig. 3(a), both G' and G'' rise with increasing angular frequency. AC enhances both the moduli of the TPEE, with the enhancement becoming more pronounced as the AC content increases. This behavior is primarily due to the improved stiffness of the matrix caused by the uniformly dispersed AC particles, which impart a higher load-bearing capacity. In addition, the

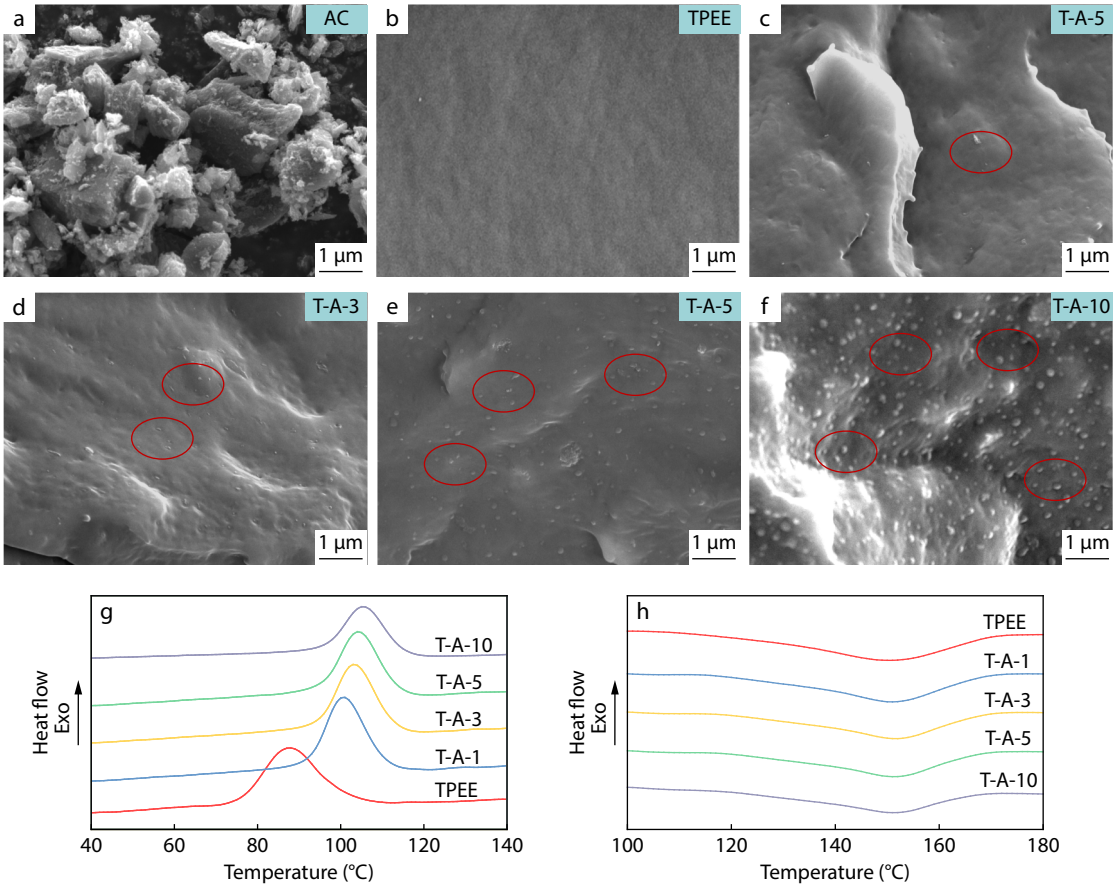

Fig. 2 The phase morphology of (a) AC, (b) TPEE, (c) T-A-1, (d) T-A-3, (e) T-A-5, (f) T-A-10; (g) The first cooling curves, and (h) second heating curves of the TPEE/AC composites.

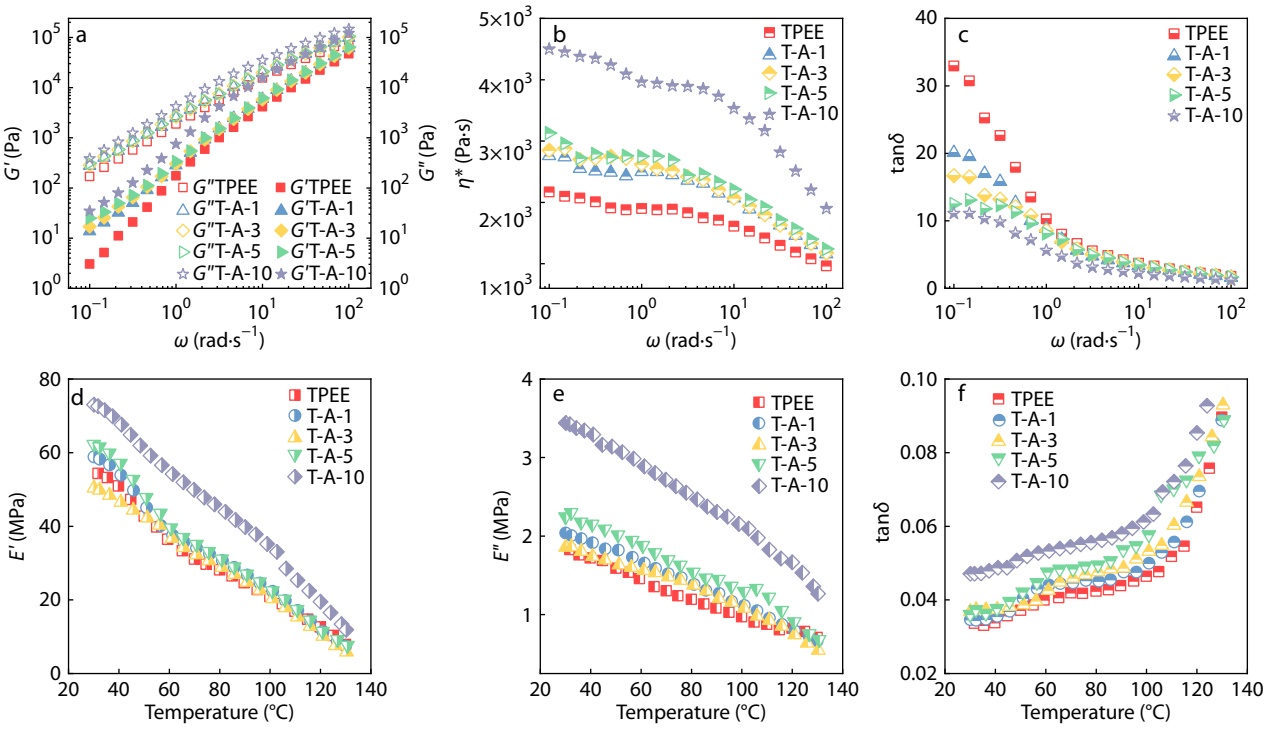

Fig. 3 The rheological behavior of TPEE/AC composites: (a) G' and G'', (b) η^*, (c) tanδ, dynamic thermodynamic response of TPEE/AC composites: (d) E', (e) E'' and (f) tanδ.

presence of physical adsorption and mechanical entanglement between AC particles and TPEE molecular chains increases interfacial energy dissipation under external forces. Furthermore, the porous structure of AC may allow partial penetration of flexible TPEE chains into its pore network. This could generate a mechanical interlocking effect, effectively anchoring the polymer chains within the porous structure. Fig. 3(b) clearly demonstrates that increasing the shear frequency leads to a reduction in η^*, which is a characteristic feature of shear-thinning materials. Meanwhile, the progressive incorporation of AC limits the flexibility of the soft TPEE segments, thereby causing a notable viscosity increase. As illustrated in Fig. 3(c), the tanδ decreases significantly with increasing angular frequency, with a more pronounced decline observed at low frequencies compared to high frequencies. This indicates a transition tendency of the composite's rheological behavior from liquid-like to solid-like. Moreover, as the AC content increases, the loss tangent gradually decreases, suggesting that the addition of AC enhances the melt elasticity of TPEE and improves its resistance to deformation at elevated temperatures.

Dynamic mechanical analysis (DMA) is a technique used to research the dynamic thermodynamic response of polymers subjected to stress. Figs. 3(d)–3(f) illustrate the temperature-dependent variations in storage modulus (E'), loss modulus (E''), and tanδ for TPEE/AC composites. According to the figures, an elevated temperature-induced reduction in both E' and E'' is observed for the TPEE/AC composites. Notably, all composites exhibit a higher modulus than pure TPEE above 50 °C. The observed enhancement in TPEE modulus upon AC incorporation aligns well with the results of the preceding rheological analysis. Interestingly, the loss factor (tanδ) obtained from rheological and DMA tests exhibits opposite trends, revealing the differential influence of AC fillers on the viscoelastic properties of TPEE under distinct testing conditions. During rheological measurements in the molten state at 180 °C, the TPEE molecular chains possess high mobility. The incorporation of AC increases the rigidity of the composite system and restricts the motion of chain segments, thereby significantly enhancing the storage modulus and reducing the tanδ. In contrast, during DMA testing within the 30–130 °C range, where the material exists in a rubbery state with limited chain mobility and relatively high modulus, the interfacial friction and energy dissipation between AC and TPEE molecular chains become more pronounced. This leads to an increased loss modulus and a markedly elevated tanδ. These findings demonstrate that the viscoelastic response of polymer composites to filler addition is strongly temperature-dependent and state-sensitive, offering theoretical insight for the rational design of processing conditions and performance optimization in practical applications. Furthermore, the tanδ curve of pure TPEE crosses over and exceeds that of the TPEE/AC composites at 120 °C, aligning well with the prior analysis. It can be concluded that AC plays a crucial role in reinforcing the melt strength of TPEE. This enhancement in viscoelasticity and melt strength help prevent cellular rupture and gas escape during the foaming process, thereby enhancing the overall foaming performance.

Foaming Behavior

The diffusion and solubility of gas in thermoplastic polymers exert a direct influence on the nucleation and subsequent expansion of foam cells.[25,26] The solubility and desorption diffusion coefficients of the TPEE/AC composites were investigated as functions of saturation time through adsorption-desorption

tests conducted at 15 MPa and 125 °C, as shown in Fig. 4. As demonstrated in Fig. 4(a), the CO_2 solubility initially increased rapidly with adsorption time and gradually reached equilibrium after 50 min of saturation. This observation suggests that gas saturation in the polymer is achieved after 50 min of adsorption, which facilitates the formation of TPEE foams with uniform cellular structures. Consequently, a foaming duration of 50 minutes is selected. As shown in Fig. 4(b), the equilibrium solubility of CO_2 initially increases with rising AC content, followed by a subsequent decrease at higher content. The solubility of CO_2 in TPEE is 7.23%, while that in T-A-5 is 7.72%, representing an increase of 6.8%. This phenomenon can be ascribed to the strong CO_2 adsorption capability of AC, which stems from its highly porous structure and large specific surface area. Nevertheless, excessive AC content results in elevated melt strength, hindering CO_2 solubility and diffusivity. Moreover, as AC content rises, the diffusion coefficient of the composites initially increases slightly and then decreases. At low AC contents, the porous structure of AC provides additional diffusion pathways for CO_2. However, as the content increases, AC begins to agglomerate and the particle size grows, as previously described, which creates macroscopic barriers to CO_2 diffusion. In addition, the enhancement of TPEE melt strength by AC further inhibits CO_2 diffusion.

Figs. 4(c) and 4(d) present the initial and final expansion ratio of TPEE/AC composites under 15 MPa. It is observed that while the initial expansion ratio of TPEE is reduced by the presence of AC, a suitable AC content facilitates an increase in the final expansion ratio. The adsorption effect of AC on polymer chains restricts chain mobility and enhances TPEE's melt strength, suppressing bubble growth and thus decreases the initial expansion ratio. On the other hand, this effect effectively controls TPEE's shrinkage, thus contributing to a higher final expansion ratio. However, this same effect mitigates the shrinkage behavior of TPEE, thereby improving its final expansion ratio. The maximum expansion ratio of pure TPEE is 13.8, while that of T-A-5 reaches 16.0, representing an increase of 15.9%. Fig. 4(e) shows TPEE/AC foams' cell diameter and cell density at a fixed expansion ratio of 13. With increasing AC content, smaller cell sizes and higher cell densities are observed, suggesting that AC enhances cell nucleation and refines the cellular morphology. Figs. 4(f)–4(i) present the corresponding cell morphology of the composite foams.

Shrinkage and Recovery Behavior

The shrinkage and recovery behaviors are inherent characteristics of elastomeric foams, and their investigation is crucial for

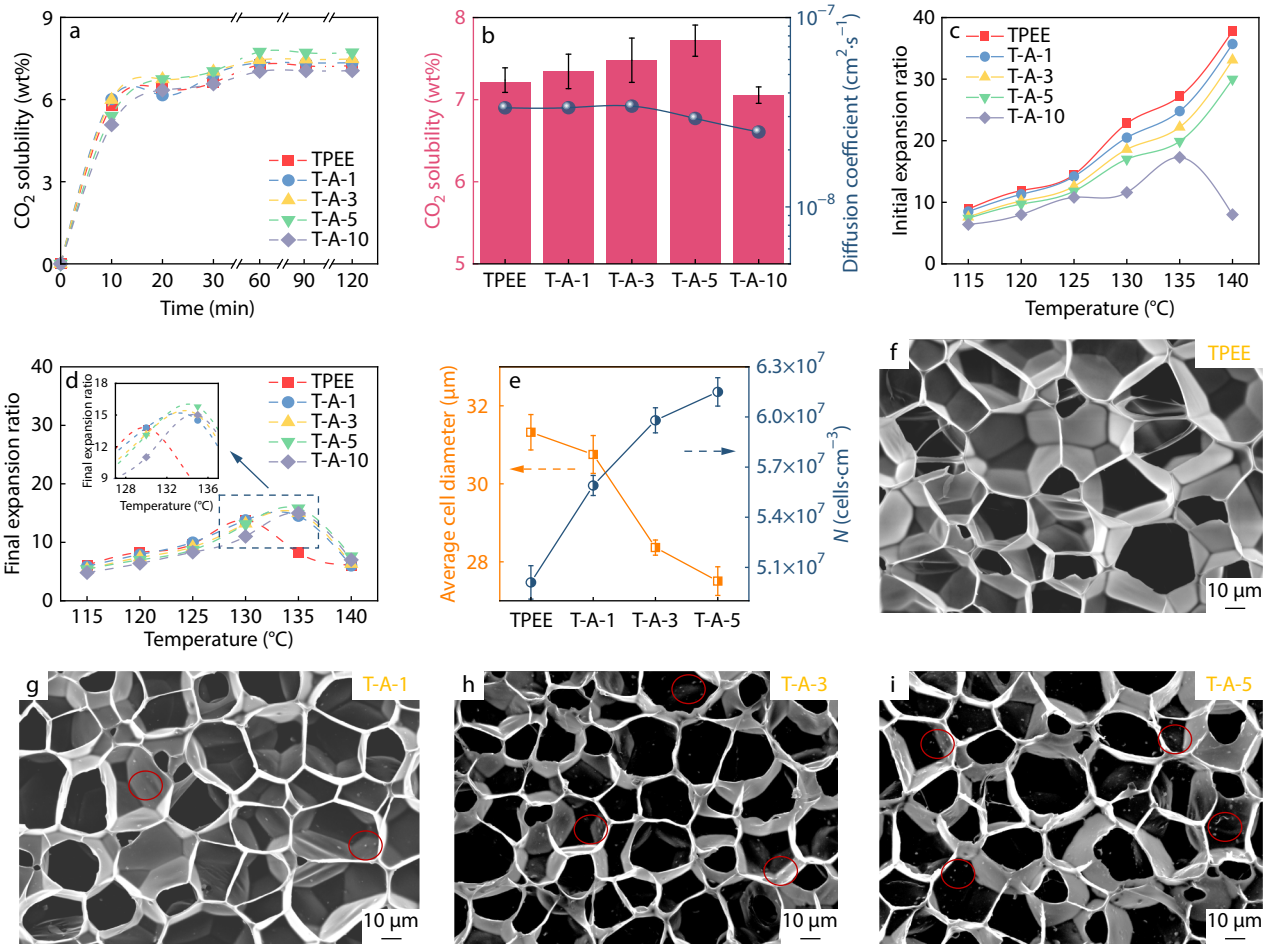

Fig. 4 Sorption and desorption tests of TPEE/AC composites: (a) relationship between solubility and adsorption time, and (b) CO_2 solubility and diffusion coefficient, (c) initial expansion ratio, and (d) final expansion ratio prepared under 15 MPa, (e) cell diameter and cell density of TPEE/AC foams at an expansion ratio of 13, the morphology of TPEE/AC foams: (f) TPEE, (g) T-A-1, (h) T-A-3, and (i) T-A-5.

https://doi.org/10.1007/s10118-026-3641-6

the fabrication of ultralight, highly resilient, and multifunctional TPEE foams. Figs. 5(a)–5(c) present the time-dependent evolution of the expansion ratio over time under 15 MPa. A shrinkage-recovery trend is observed, where the expansion ratio exhibits an initial decline followed by a gradual increase. This trend becomes more pronounced at higher foaming temperatures. In addition, TPEE/AC foams' expansion ratio initially decreases, reaching a minimum after 5 h of standing, followed by a gradual increase over the course of 14 days until reaching a stable state. To further quantify TPEE/AC foams' shrinkage and recovery characteristics, Figs. 5(d)–5(i) illustrate the initial, post-shrinkage, and post-recovery expansion ratio, corresponding shrinkage rate (*S*) and recovery ratio (*R*) of the composite foams fabricated at different temperatures. At foaming temperatures below 135 °C, the pure TPEE foam exhibits a relatively lower shrinkage rate and improved recovery compared to that at 135 °C. This behavior can be attributed to the dominant role of hard-segment crystallization at lower temperatures. At low temperatures, the hard-segment crystalline domains in neat TPEE act as effective physical cross-linking points, providing structural stability to the cell walls and thereby reducing shrinkage. As the foaming temperature increases, the hard-segment crystalline domains gradually melt, leading to a decrease in the melt strength of TPEE, which is unfavorable for maintaining structural stability. Moreover, the presence of hard-segment crystalline domains at low temperatures restrains cell growth, resulting in a lower initial expansion ratio, which further contributes to the reduced shrinkage behavior of TPEE foam. The incorporation of AC effectively reduces shrinkage and enhances the recovery performance of TPEE foams. Under the foaming condition of 135 °C, the pure TPEE foam exhibits a final expansion ratio of 8.0, an *S* of 79.8%, and a *R* of 25.4%. In contrast, the T-A-5 foam achieves a final expansion ratio of 16.0, with an *S* of 70.0% (a 12.3% reduction), and a *R* of 79.4%, representing a 212.6% improvement. Furthermore, the T-A-10 foam shows a final expansion ratio of 15.0, an *S* of 47.0% (a 41.1% improvement), and a *R* of 89.0%, corresponding to a 250.4% increase over pure TPEE foams. For pure TPEE foams, the molecular chains possess high mobility, making it easy to achieve a high initial expansion ratio. This typically results in large cells and thin walls. Owing to the insufficient mechanical stability of the bubble walls and the continuous diffusion of CO_2 to the surroundings, the foams tend to shrink.[27] Moreover, during the evolution of cellular structure, the bubble walls undergo multidirectional stretching, which disrupts physical entanglements of molecular chains and leads to severe relaxation, thereby limiting the increase in expansion ratio during the recovery process. In contrast, incorporating AC into the TPEE induces a heterogeneous nucleation mechanism, leading to the generation of smaller and more uniformly distributed cells, thereby enhancing the robustness of the cellular framework. Additionally, the adsorption of AC on TPEE molecular chains provides physical

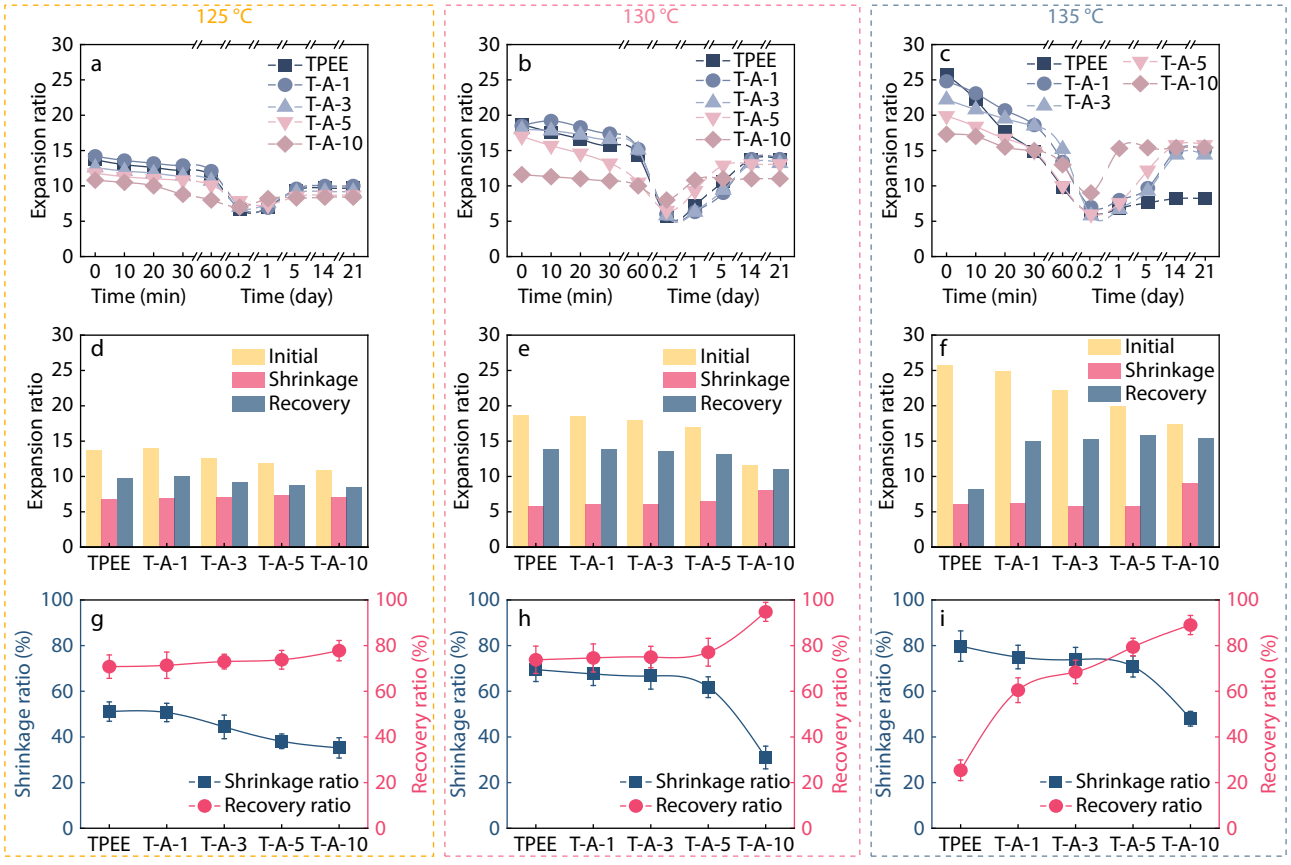

Fig. 5 Changes in expansion ratio of TPEE/AC foams fabricated at 15 MPa across various temperatures: (a) 125 °C, (b) 130 °C, and (c) 135 °C, the expansion ratio at three stages for foams prepared at (d) 125 °C, (e) 130 °C, and (f) 135 °C, the shrinkage and recovery rate of TPEE/AC foams prepared at (g) 125 °C, (h) 130 °C, and (i) 135 °C.

https://doi.org/10.1007/s10118-026-3641-6

support, enhancing the resistance of the chains to deformation and improving their recovery ability. Consequently, TPEE/AC foams exhibit a lower shrinkage rate and an enhanced recovery rate. The mechanism diagram is provided in Fig. 6.

Blackness and Compressive Properties

In foam applications and manufacturing industries, color control is a critical parameter, with the blackness value being a vital indicator for evaluating color quality. Figs. 7(a)–7(c) show the apparent color band images, lightness values, and blackness values of TPEE/AC composites and their foams with various expansion ratio. With increasing expansion ratio, the foams exhibit lighter coloration, higher lightness values, and lower blackness values. As the expansion ratio increases, the content of AC per unit volume decreases. The excessively dispersed AC reduces the visible light absorption and scattering capability of the polymer, thereby leading to a decrease in blackness. As AC content increases, TPEE/AC foams appear darker, with reduced lightness and increased blackness values.

Cyclic compressive performance is a crucial parameter for assessing the practical applicability of elastomeric foams. Compressive strength is indicative of the material's ability to withstand external forces, while energy loss coefficient ($\Delta U/U$) serves as a measure of elastic recovery performance. A low energy loss coefficient implies superior elasticity, indicating that the foam can rapidly recover its original shape after deformation. As illustrated in Figs. 7(d)–7(f), the 20-cycle compressive curves of TPEE/AC foams exhibit considerable overlap, indicating exceptional toughness and elasticity. Furthermore, the addition of AC significantly enhances the composite foams' resistance to external compression compared to pure TPEE foam. Fig. 7(g) presents the specific data on maximum compressive stress (σ_{max}) and $\Delta U/U$ of TPEE/AC foams. Compared to the pure TPEE foam, the addition of AC endows the composite foams with higher σ_{max} and lower $\Delta U/U$. The average maximum stress of pure TPEE foam is 0.17 MPa with an energy loss coefficient of 0.153. For the T-A-1 foam, the

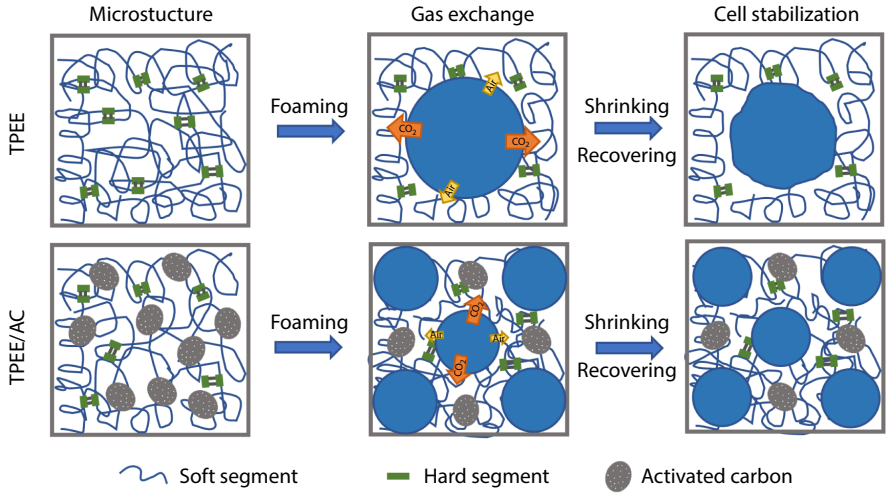

Fig. 6 Mechanism diagram of shrinkage and recovery behavior.

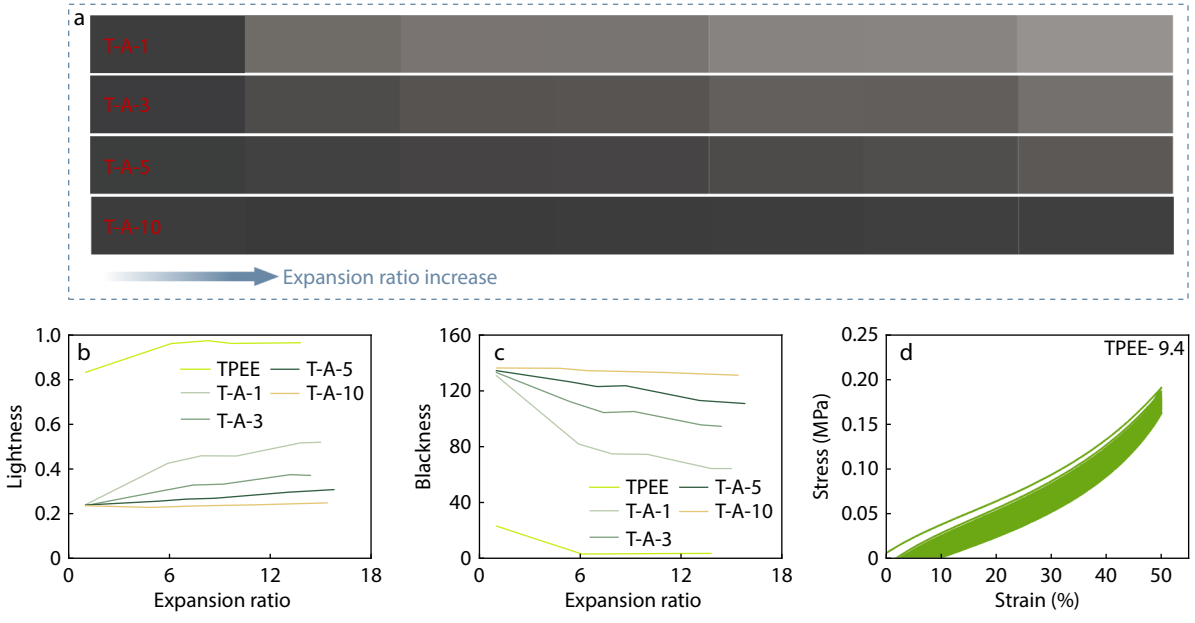

https://doi.org/10.1007/s10118-026-3641-6

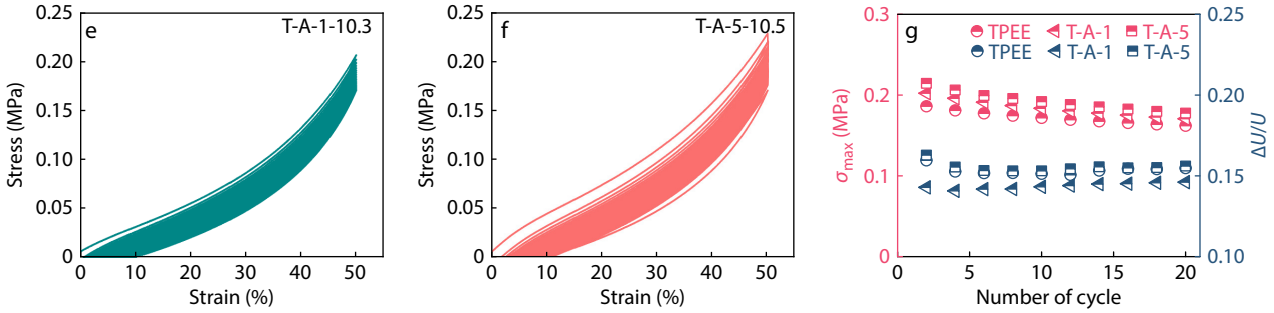

Fig. 7 TPEE/AC composites and foams: (a) the apparent color band images, (b) lightness, (c) blackness, stress-strain response of (d) TPEE foam, (e) T-A-1 foam and (f) T-A-1 foam, (g) TPEE/AC foams' σ_{max} and $\Delta U/U$.

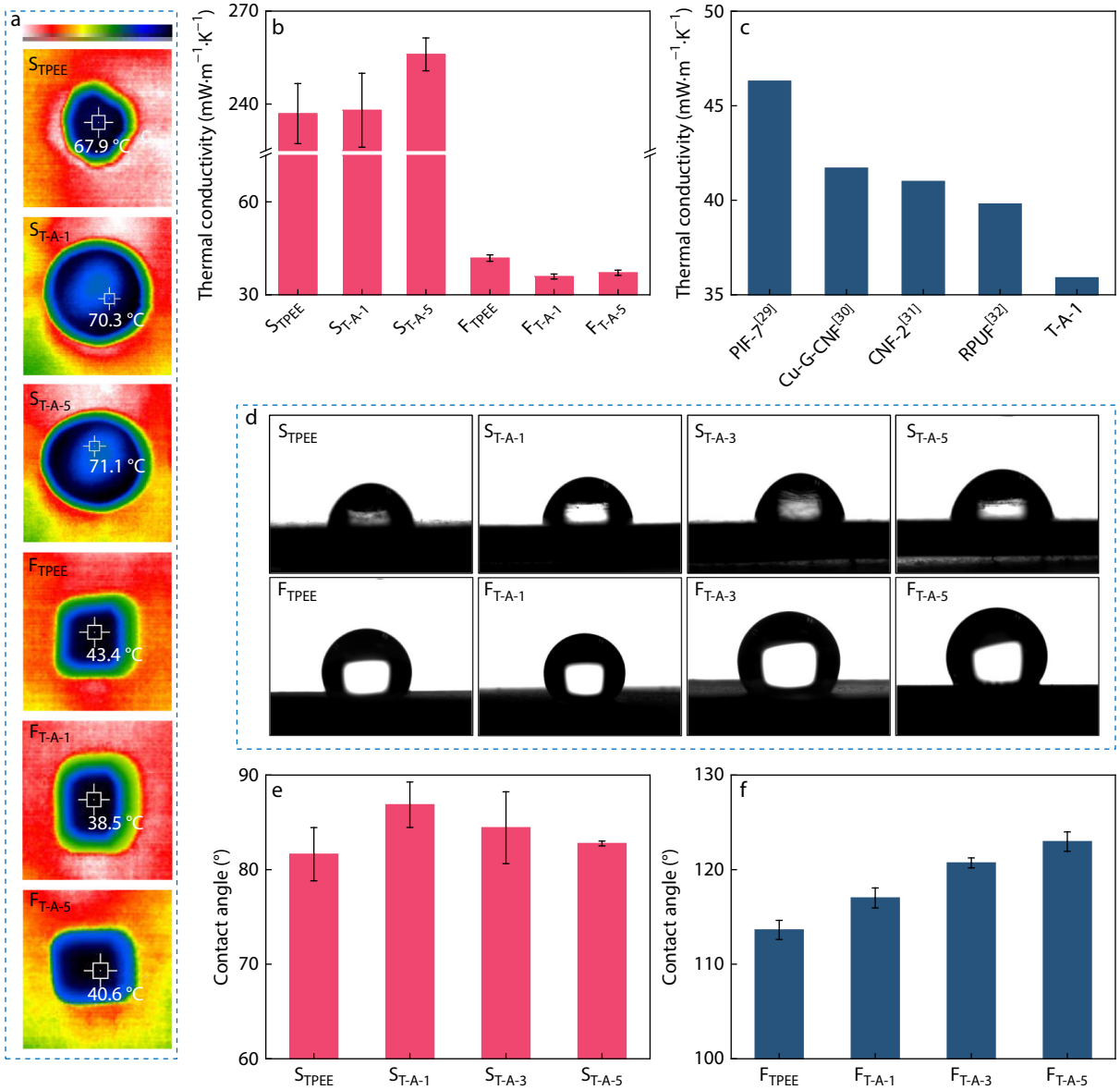

Fig. 8 TPEE/AC composites and their foams with maximum foaming ratio: (a) infrared thermal images, (b) thermal conductivity, (c) the comparison with other thermal insulating materials, (d) hydrophobic pictures, water contact angle values of (e) TPEE/AC composites, and (f) TPEE/AC foams with an expansion ratio of 7.

maximum stress reaches 0.18 MPa and the energy loss coefficient drops to 0.144, representing an 8.2% increase in strength and a 5.9% decrease in energy dissipation, respectively. The T-A-5 foam exhibits an even higher maximum

stress of 0.19 MPa, corresponding to an 11.8% improvement. In addition, the expansion ratio of all tested composite foams is slightly higher than pure TPEE foam, further confirming the significant enhancement in compressive performance induced by AC addition. As a rigid filler with high modulus, AC can serve as an effective stress-bearing site within the TPEE matrix. Moreover, the adsorption of TPEE molecular chains by AC reduces chain yielding and relaxation, which contributes to improved stability of the foam cell walls.

Thermal Insulation and Hydrophobicity

Given the importance of thermal insulation in reducing energy consumption and emissions, Fig. 8(a) displays the infrared thermography of TPEE/AC composites and their corresponding foams with the highest expansion ratios to provide a visual comparison of their insulation performance. It can be observed that upon heating on an 80 °C platform for 5 min, the temperatures of TPEE/AC foams are significantly lower than that of the unfoamed TPEE/AC composites. The surface temperature of the solid TPEE reaches 67.9 °C, whereas that of the T-A-1 foam is only 38.5 °C, showing a 50.7% reduction. To provide a more quantitative evaluation of heating insulation properties, the thermal conductivity (K_t) values of aforementioned materials are illustrated in Fig. 8(b). The unfoamed TPEE exhibits a K_t of 236.7 $mW{\cdot}m^{-1}{\cdot}K^{-1}$, which decreases to 41.8 $mW{\cdot}m^{-1}{\cdot}K^{-1}$ upon foaming. Further incorporation of AC leads to a reduction in K_t of the T-A-1 foam to 35.9 $mW{\cdot}m^{-1}{\cdot}K^{-1}$, reflecting an 84.8% reduction relative to the TPEE solid and a 14.1% decrease compared to the TPEE foam. The significant reduction in K_t highlights the effective role of AC in improving the TPEE foams' heating insulation properties. This improvement can be attributed to the introduction of a large amount air with low thermal conductivity into the TPEE matrix during foaming. The rise in expansion ratio results in a noticeable decline in the solid-phase thermal conductivity.[28] Furthermore, the carbon-based filler AC enhances the infrared radiation attenuation capability of the polymer matrix, which is conductive to reducing radiative conductivity of TPEE foam. Compared with previously reported thermal insulating materials, the TPEE/AC foams developed in this study exhibit lower thermal conductivity and excellent insulation performance, greatly enhancing their potential applications in heat preservation, as depicted in Fig. 8(c). [29–32] The hydrophobicity of foams plays a crucial role in reducing moisture-induced degradation of thermal insulation performance and prolonging service life. Fig. 8(d) presents the water contact angle (WCA) images of TPEE/AC composites and their corresponding foams (with a foaming ratio of 7), while the specific values are shown in Figs. 8(e) and 8(f). The data clearly indicate a significant enhancement in hydrophobicity of TPEE/AC composites following the foaming process. The WCA of the solid TPEE is 81.6°, while that of the T-A-5 foam reaches 122.5°, representing a 50.2% increase compared to the solid TPEE. Moreover, as the AC content increases, the WCA of TPEE/AC foams also gradually increases. This enhancement mainly results from the cell size refinement effect induced by AC. The reduction in cell size improves the material's ability to resist water droplet penetration, making it more difficult for water to infiltrate the foam, thereby exhibiting superior hydrophobic performance.

CONCLUSIONS

In summary, lightweight, high-strength and elastic TPEE/AC foams with excellent hydrophobicity and heating insulation were successfully prepared using a simple and environmentally friendly microcellular foaming technology. AC demonstrated good dispersion within the TPEE matrix and exhibited favorable interfacial compatibility. Its incorporation increased both the melting and crystallization temperatures of TPEE. Viscoelastic properties of TPEE/AC composites tested under two different conditions revealed contrasting trends in loss factor, indicating that the influence of fillers on polymer viscoelasticity is highly temperature-dependent and state-sensitive. The porous structure and large specific surface area of AC facilitate strong CO_2 adsorption, thereby enhancing the CO_2 solubility in TPEE. Furthermore, the interaction between AC and TPEE molecular chains increased the melt strength of TPEE, improved foaming behavior, and contributed to a more refined cellular structure. AC also effectively reduced the shrinkage ratio and enhanced the recovery ratio of TPEE. The T-A-5 foam achieved a final expansion ratio of 16.0, a shrinkage ratio of 70.0%, and a recovery ratio of 79.4%, representing improvements of 15.9%, 12.3%, and 212.6%, respectively, compared to pure TPEE foam, demonstrating excellent application potential. Further, it was demonstrated that both lightness and blackness of the TPEE/AC composite foams can be tailored by varying AC content and manipulating cellular morphology. Additionally, the addition of AC contributed to a substantial enhancement in the mechanical properties of TPEE foam, characterized by higher maximum compressive stress and lower energy loss coefficient. The prepared TPEE/AC foams also exhibited outstanding thermal insulation and hydrophobic properties, with a low thermal conductivity of 35.9 $mW{\cdot}m^{-1}{\cdot}K^{-1}$ and a water contact angle of 122.5°. This research offers a promising strategy for the development of high-performance thermoplastic polyester elastomer foams, providing new insights into lightweight, multifunctional materials for energy efficient and environmental protection applications.

Conflict of Interests

The authors declare no interest conflict.

Electronic Supplementary Information

Electronic supplementary information (ESI) is available free of charge in the online version of this article at http://doi.org/10.1007/s10118-026-3641-6.

Data Availability Statement

The data that support the findings of this study are available from the corresponding author upon reasonable request.

ACKNOWLEDGMENTS

This work was financially supported by the National Natural Science Foundation of China (No. 52175341), Shandong

Provincial Natural Science Foundation (No. ZR2022JQ24), Funding Project of Jinan City's New Twenty Items for Colleges and Universities (No. 202333038), Excellent Young Team Project of Central Universities (No. 2023QNTD002), and Qingdao Key Technology Research and Industrialization Demonstration Project (No. 24-1-2-qljh-10-gx).

REFERENCES

1 Yang, T.; Zuo, J.; Liu, F.; Liu, C.; Chen, C.; Jiang, X.; Liu, K.; Yu, S.; Wang, J.; Zhu, J. Bio-based thermoplastic poly(ether-ester) elastomers from 2,5-thiophenedicarboxylic acid with high stiffness and elasticity. *Chem. Eng. J.* **2025**, *510*, 161856.
2 Zhang, J. W.; Liu, F.; Wang, J. G.; Na, H. N.; Zhu, J. Synthesis of poly(butylene terephthalate)-poly(tetramethylene glycol) copolymers using terephthalic acid as starting material: a comparation between two synthetic strategies. *Chinese J. Polym. Sci.* **2015**, *33*, 1283–1293.
3 Tang, S.; Li, J.; Wang, R.; Zhang, J.; Lu, Y.; Hu, G. H.; Wang, Z.; Zhang, L. Current trends in bio-based elastomer materials. *SusMat* **2022**, *2*, 2–33.
4 Sono, M.; Kinashi, K.; Sakai, W.; Tsutsumi, N. Spin-trapping analysis and characterization of thermal degradation of thermoplastic poly(ether–ester) elastomer. *Macromolecules* **2018**, *51*, 1088–1099.
5 Nagai, Y.; Ogawa, T.; Zhen, L. Y. Analysis of weathering of thermoplastic polyester elastomers—I. polyether-polyester elastomers. *Polym. Degrad. Stabil.* **1997**, *56*, 115–121.
6 Hopmann, C.; Lemke, F.; Nguyen Binh, Q. Foaming of EPDM with water as blowing agent in injection molding. *J. Appl. Polym. Sci.* **2016**, *133*, 43613.
7 Chang, C. T.; Kuo, K. C.; Ho, J. H.; Lee, L. R.; Gautam, B.; Ciou, J. H.; Tseng, Y. H.; Chang, C. W.; Wu, C. T.; Lin, C. T. Reversible sensing technologies using upcycled TPEE: crafting pH and light responsive materials towards sustainable monitoring. *Small*

Graphical Abstract

Activated Carbon-derived Polyester Elastomer Foams with Tailored Structure and Blackness for High-performance Thermally Insulating Applications

Xu-Jiang Sun, Yan-Ru Zhang, Jia-Peng Ma, Xu Wang, Ke-Jian Cui, Ting-Ting Feng, and Gui-Long Wang

Shandong University; Shandong Special Equipment Inspection Institute Group Co., Ltd.; Li Ning (China) Sports Goods Co., Ltd.

A green microcellular foaming strategy with activated carbon produces lightweight TPEE foams featuring refined cells, reduced shrinkage, high recovery, low thermal conductivity, enhanced strength, and hydrophobic surfaces.

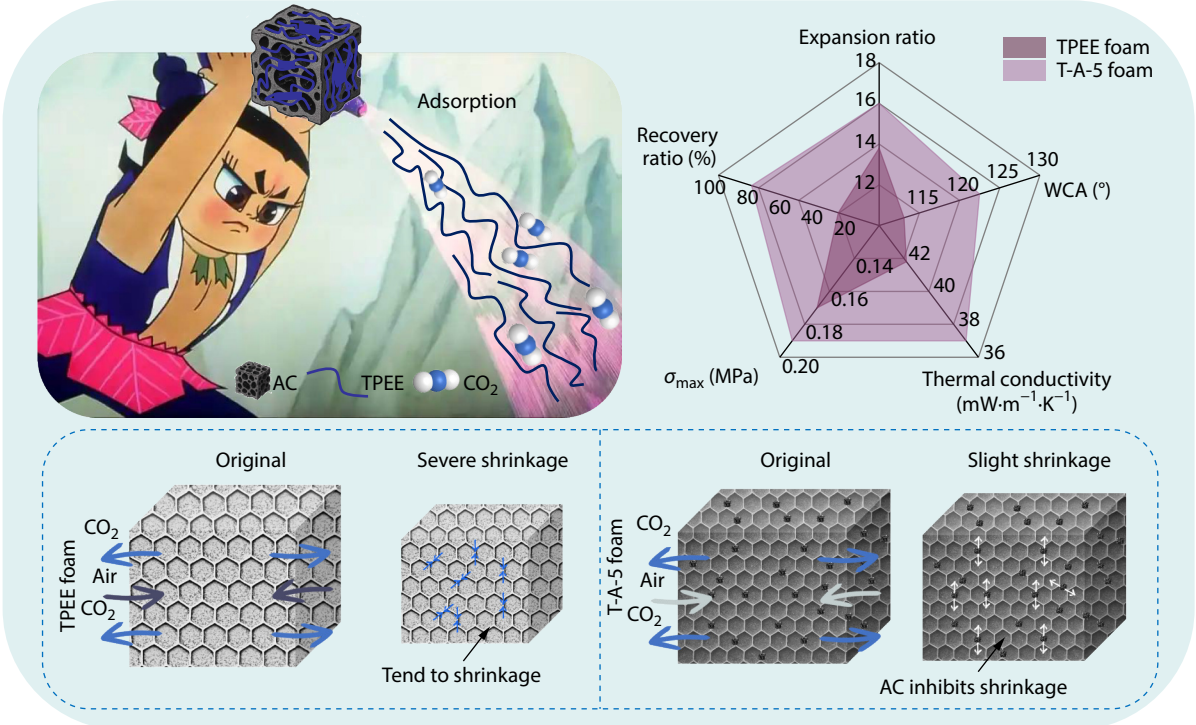

Chinese J. Polym. Sci. 2026, 44, 2258–2268 *https://doi.org/10.1007/s10118-026-3641-6*

2024, *20*, 2400491.
8 Ranganathan, P.; Chen, C. W.; Chou, Y. L.; Rwei, S. P.; Ramaraj, S. K. Biomass chemical upcycling of waste rPET for the fabrication of formamide-free TPEE microcellular foams via $scCO_2$ foaming. *J. CO_2. Util.* **2022**, *65*, 102199.
9 Xu, Z.; Wang, G.; Zhang, A.; Sun, X.; Zhao, G. Thermoplastic polyester elastomer foams with tailored morphology and mechanical performance achieved by manipulating microphase-separated structure. *Chem. Eng. J.* **2025**, *509*, 161191.
10 Cao, Y.; Pang, Y.; Dong, X.; Wang, D.; Zheng, W. To clarify the resilience of PEBA/MWCNT foams via revealing the effect of the nanoparticle and the cellular structure. *ACS. Appl. Polym. Mater.* **2021**, *3*, 3766–3775.
11 Wang, G.; Dong, M.; Deng, H.; Ma, X.; Zhu, B.; Zhou, L.; Zhang, X.; Tan, D.; Algadi, H. Polypropylene foaming using supercritical carbon dioxide: a review on fundamentals, technology, and applications. *Adv. Compos. Hybrid. Mater.* **2025**, *8*, 84.
12 Wei, C.; Chai, J. L.; Li, S.; Wang, G. L. Microcellular foaming-derived superlight ultra-high molecular weight poly(vinylidene fluoride) foams for outstanding thermal insulation applications. *Chinese J. Polym. Sci.* **2025**, *43*, 1837–1849.
13 Yu, S.; Liu, Y.; Hao, M.; Zhang, X.; Zhang, X.; Yuan, Y.; Zhang, Z. Ultrahigh electromagnetic interference shielding and integrated thermal sensing-encryption enabled by a honeycomb-inspired multifunctional foam. *Chinese J. Polym. Sci.* **2026**, *44*, 513–524.
14 Sun, X.; Wang, G.; Xu, Z.; Chai, J.; Zhang, A.; Zhao, G.; Li, S.; Wang, Y.; Jiao, H. Microcellular foaming-derived strong ultra-high molecular weight polyethylene/high-density polyethylene foams for thermally insulating and oil-water separating applications. *J. Environ. Chem. Eng.* **2024**, *12*, 113992.
15 Xu, M.; Wei, L.; Ma, L.; Lu, J.; Liu, T.; Zhang, L.; Zhao, L.; Park, C. B. Microcellular foamed polyamide 6/carbon nanotube composites with superior electromagnetic wave absorption. *J. Mater. Sci. Technol.* **2022**, *117*, 215–224.
16 Wu, D.; Xie, W.; Wang, Z.; Peng], S. Thermoplastic polyester elastomer composites containing two types of filler particles with different dimensions: structure design and mechanical property control. *Compos. Struct.* **2018**, *197*, 21–27.
17 Xu, Z.; Wang, G.; Zhao, J.; Zhang, A.; Dong, G.; Zhao, G. Anti-shrinkage, high-elastic, and strong thermoplastic polyester elastomer foams fabricated by microcellular foaming with CO_2 & N_2 as blowing agents. *J. CO_2. Util.* **2022**, *62*, 102076.
18 Sun, X.; Wang, G.; Xu, Z.; Li, X.; Ma, C.; Zhao, G. A novel synergistic enhancement for UHMWPE foam via HDPE homologous reinforcement and MWCNTs-induced "window-broken" effect for advanced biphasic separation and heating insulation. *Adv. Compos. Hybrid. Mater.* **2025**, *9*, 20.
19 Hou, H. H.; He, X.; Ma, H.; Zhou, H. F.; Wen, B. Y.; Wang, X. D.; Deng, Y. F. Lightweight ethylene-vinyl acetate copolymer/low-density polyethylene/carbon nanotube foams via supercritical carbon dioxide foaming for piezoresistive sensors. *Chinese J. Polym. Sci.* **2025**, *43*, 1208–1221.
20 Sun, X.; Wang, G.; Xu, Z.; Wang, Z.; Zhao, G. Advanced fabrication of ultra-high molecular weight polyethylene/graphite nanoplates foam for enhanced oil–water separation and thermal insulation via a novel omnidirectional gas escape barrier mechanism. *Chem. Eng. J.* **2025**, *503*, 158360.
21 Aso, O.; Eguiazábal, J.; Nazábal, J. The influence of surface modification on the structure and properties of a nanosilica filled thermoplastic elastomer. *Compos. Sci. Technol.* **2007**, *67*, 2854–2863.
22 Chen, J.; Lv, Q.; Wu, D.; Yao, X.; Wang, J.; Li, Z. Nucleation of a thermoplastic polyester elastomer controlled by silica nanoparticles. *Ind. Eng. Chem. Res.* **2016**, *55*, 5279–5286.
23 Lahuri, A. H.; Khai, M. L. N.; Rahim, A. A.; Nordin, N. Adsorption kinetics for CO_2 capture using cerium oxide impregnated on activated carbon. *Acta Chim. Slov* **2020**, *67*, 570–580.
24 Wang, J.; Pu, Q.; Ning, P.; Lu, S. Activated carbon-based composites for capturing CO_2: a review. *Greenh. Gases.* **2021**, *11*, 377–393.
25 Dong, M.; Wang, G.; Zhang, X.; Tan, D.; Ren, J.; Colorado, H.; Hou, H.; Toktarbay, Z.; Guo, Z. An overview of polymer foaming assisted by supercritical fluid. *Adv. Compos. Hybrid. Mater.* **2023**, *6*, 207.
26 Gong, Z.; Chen, Y.; Yuan, J.; Zhao, L.; Hu, D. Shape memory temperature-tunable poly (butylene adipate-co-terephthalate)/polylactic acid foams prepared by supercritical CO_2 foaming. *ACS. Sustain. Chem. Eng.* **2024**, *12*, 12064–12075.
27 Pinto, J.; Reglero-Ruiz, J. A.; Dumon, M.; Rodriguez-Perez, M. A. Temperature influence and CO_2 transport in foaming processes of poly(methyl methacrylate)–block copolymer nanocellular and microcellular foams. *J. Supercrit. Fluid.* **2014**, *94*, 198–205.
28 Hamada, H. M.; Shi, J.; Abed, F.; Humada, A. M.; Majdi, A. Recycling solid waste to produce eco-friendly foamed concrete: A comprehensive review of approaches. *J. Environ. Chem. Eng.* **2023**, *11*, 111353.
29 Yun, S.; Sheng, X.; Xiong, Z.; Ma, Z.; Qin, J.; Zhang, G. Lightweight and highly heat-resistant copolymerized polyimide foams for superior thermal insulation and acoustic absorption. *Mater. Today Phys.* **2024**, *49*, 101578.
30 Chen, C.; Zhou, Y.; Xie, W.; Meng, T.; Zhao, X.; Pang, Z.; Chen, Q.; Liu, D.; Wang, R.; Yang, V. Lightweight, thermally insulating, fire-proof graphite-cellulose foam. *Adv. Funct. Mater.* **2023**, *33*, 2204219.
31 Ren, Q.; Li, W.; Cui, S.; Ma, W.; Zhu, X.; Wu, M.; Wang, L.; Zheng, W.; Semba, T.; Ohshima, M. Improved thermal insulation and compressive property of bimodal poly (lactic acid)/cellulose nanocomposite foams. *Carbohyd. Polym.* **2023**, *302*, 120419.
32 Fu, Y.; Qiu, C.; Ni, L.; Ye, H.; Zou, H.; Luo, Y.; Liang, M. Cell structure control and performance of rigid polyurethane foam with lightweight, good mechanical, thermal insulation and sound insulation. *Constr. Build. Mater.* **2024**, *447*, 138068.